Electronic Supplementary Material (ESI) for Journal of Materials Chemistry A.

Supplementary Material

New Understanding of Crystal Control and Facet Selectivity of TiO_2 Ruling Photocatalytic Performance

Teera Butburee[1], Papasara Kotchasarn[2], Pussana Hirunsit[1], Zhuxing Sun[3,4], Qiqun Tang[4], Pongthanawat Khemthong[1], Weradesh Sangkhun[5], Wiradej Thongsuwan[2], Pisist Kumnorkaew[1], Haiqiang Wang[4], and Kajornsak Faungnawakij[1*]

[1]National Nanotechnology Center, National Science and Technology Development Agency, 111 Thailand Science Park, Pathum Thani 12120, Thailand

[2]Materials Science Research Center, Department of Physics and Materials Science, Faculty of Science, Chiang Mai University, Chiang Mai 50200, Thailand

[3]School of Environmental Science and Engineering, Shanghai Jiao Tong University, Shanghai 200240, China

[4]Department of Environmental Engineering, Zhejiang University, Hangzhou 310058, P. R. China

[5]Division of Materials Technology, School of Energy, Environment and Materials, King Mongkut's University of Technology Thonburi, Bangkok 10140, Thailand

[*]Corresponding Author

[*]Corresponding E-mail: kajornsak@nanotec.or.th

Keywords: Facet Control, TiO_2, Crystal Growth, CO_2 Photoreduction, PEC Water Splitting

S1: Structural evolution when a trace amount of F$^-$ ions was added

Table S1 The experimental conditions for studying the effect of trace amount of F$^-$ ions on the morphology of TiO_2

Exp.	37% HCl **(mL)**	H_2O **(mL)**	TTBT **(mL)**	AFT **(g)**	Time **(h)**	Temp. **(°C)**	Factor to study
S1.1	25	35	1	**0.025**	17	150	Trace amount of F$^-$ ions
S1.2	25	35	1	**0.050**	17	150	
S1.3	25	35	1	**0.100**	17	150	

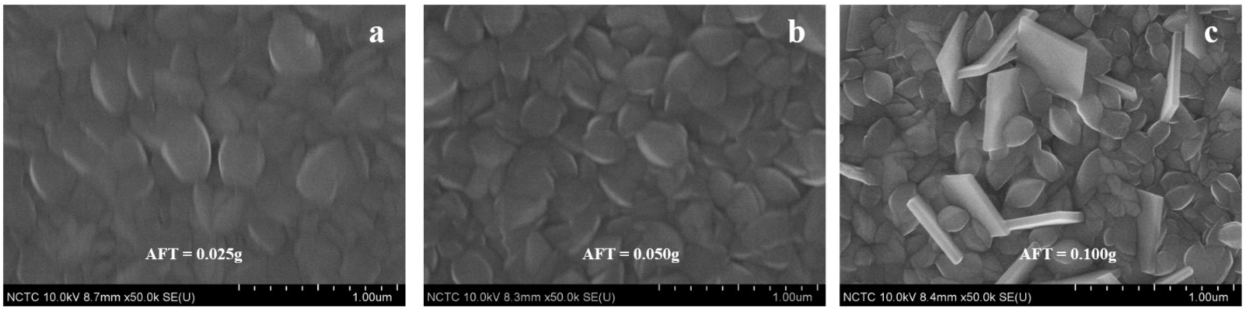

Figure S1 SEM images showing the morphology of the particles when a trace amount of F$^-$ ions was added to the system. a-c) the resultant morphology obtained from the condition S1.1-S1.3, respectively.

S2: Systematic study of the factors affecting the growth of TiO_2

Table S2 The experimental conditions for studying the factors affecting growth of TiO_2

Exp.	HCl (mL)	H_2O (mL)	TTBT (mL)	AFT (g)	Time (h)	Temp. (°C)	Factor to study
S2.0	25.0	35.0	1.00	**0.0**	24	150	Effect of F^- ions
S2.1	25.0	35.0	1.00	**0.2**	24	150	
S2.2	25.0	35.0	1.00	**0.4**	24	150	
S2.3	25.0	35.0	1.00	**0.6**	24	150	
S2.4	25.0	35.0	1.00	**0.8**	24	150	
S2.5	**25.0**	35.0	1.00	0.5	24	150	Effect of H^+ ions
S2.6	**27.5**	32.5	1.00	0.5	24	150	
S2.7	**30.0**	30.0	1.00	0.5	24	150	
S2.8	**20.0**	40.0	1.00	0.5	24	150	
S2.9	**35.0**	25.0	1.00	0.5	24	150	
S2.10	25.0	35.0	**0.50**	0.4	24	150	Effect of Ti^{4+} precursor
S2.11	25.0	35.0	**0.75**	0.4	24	150	
S2.12	25.0	35.0	**1.25**	0.4	24	150	
S2.13	25.0	35.0	**1.50**	0.4	24	150	
S2.14	25.0	35.0	1.00	0.5	10	**150**	Effect of reaction temperature
S2.15	25.0	35.0	1.00	0.5	10	**160**	
S2.16	25.0	35.0	1.00	0.5	10	**180**	
S2.17	20.0	40.0	1.00	0.5	**2**	150	Effect of reaction time
S2.18	20.0	40.0	1.00	0.5	**4**	150	
S2.19	20.0	20.0	1.00	0.5	**8**	150	

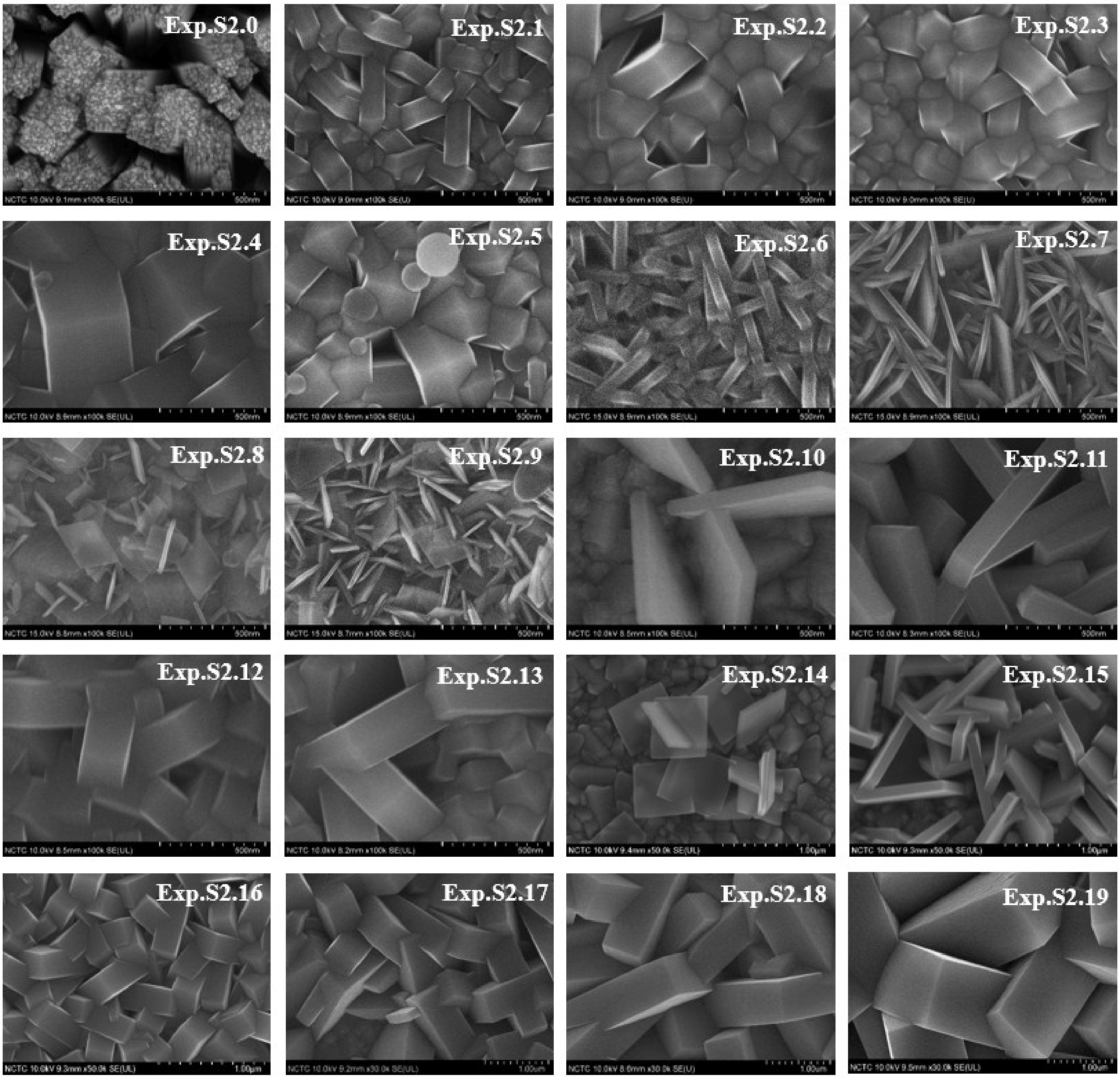

Figure S2 SEM observation of the morphology of the corresponding products from Exp.S2.0-Exp.S2.19 in Table S2.

The effect of F$^-$ ions: The effect of F$^-$ ions can be found in Exp.S2.0-Exp.S2.4. Rutile nanorods in Exp.S2.0 were changed to anatase with facets in Exp.S2.1-Exp.S2.4 when a variable amount of AFT was added to the system (discussed this phenomenon in details in the main text). Comparing Exp.S2.1-Exp.S2.4, when the amount of AFT was increased, the thickness of particles was increased. In other words, the percentage of {101} facet in the particles was increased.

The effect of H$^+$ ions: The effect of H$^+$ ions can be found in Exp.S2.5-Exp.S2.9. When compare Figure Exp.S2.5-Exp.S2.9, it was found that the particles clearly become thinner. In other words, the percentage of {001} in the particles was increased with respect to the increment of H$^+$ ions.

The effect of the amount of Ti^{4+} precursor: The effect of the amount of Ti^{4+} precursor can be found in Exp.S2.10-Exp.S2.13. As seen from Figure S2, the particles on the substrate become denser and thicker when the amount of Ti^{4+} precursor was increased.

The effect of reaction temperature: The effect of reaction temperature can be found in Exp.S2.14-Exp.S2.16. Under an identical reactant receipt, the particle size appeared to be larger when the reaction temperature was increased. However, note that the reaction temperature should be in the range of 150-180 °C. The reaction temperature outside this range causes irregular shapes.

The effect of reaction time: The effect of reaction time can be found in Exp.S2.17-Exp.S2.19. Obviously, the particles grow to a larger size when the reaction time was prolonged. However, special attention should be paid when the concentration of HCl is below 33.3 vol%, as the particles reach their full-grown quickly, and then small spherical particles grow afterward. The details can be found in section S5.

S3: Raman Spectra quantifying the percentage of {001} facet

Based on Raman vibrational modes proposed by Tian et al. [1], E_g peaks is caused by symmetric stretching vibration of O-Ti-O, while B_{1g} and A_{1g} are caused by symmetric bending and antisymmetric bending of O-Ti-O in TiO_2, respectively. On {001} facet, there are only unsaturated bonding modes such as five-coordinated Ti (5c-Ti) and two-coordinated O (2c-O), while on the other facets such as {101}, there are the mixtures of both saturated and saturated bonding modes such as six-coordinated Ti (6c-Ti), three-coordinated O (3c-O), 5c-Ti, and 2c-O. Therefore, it could say that the higher the percentage of {001} facet exposed on the surface, the lower intensity of E_g peak will be, due to the reduction of the symmetric stretching vibration modes of O-Ti-O. On the other hand, the intensity of A_{1g} and B_{1g} peaks become increased because of the more number of the symmetric bending vibration and antisymmetric bending vibration. Based on this concept, the percentage of {001} can be calculated by the following equation:

$$\%\{001\}= \frac{Intensity\ of\ A1g}{Intensity\ of\ Eg}\ \mathrm{x}\ 100 \qquad \text{Equation S1}$$

This quantifying technique is proposed as the more sensitive and accurate method as compared to the conventional XRD method [1].

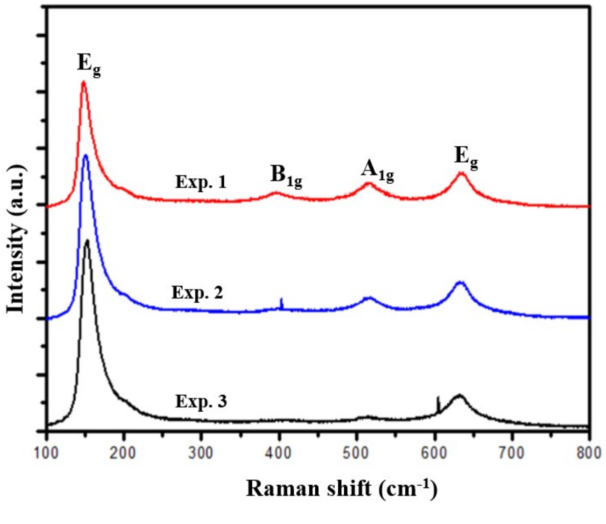

Figure S3.1 Raman spectra of Exp.1-Exp.3.

Based on Equation S1, the percentage of {001} in Exp. 1-3 is 66.53, 32.71, and 11.13%, respectively

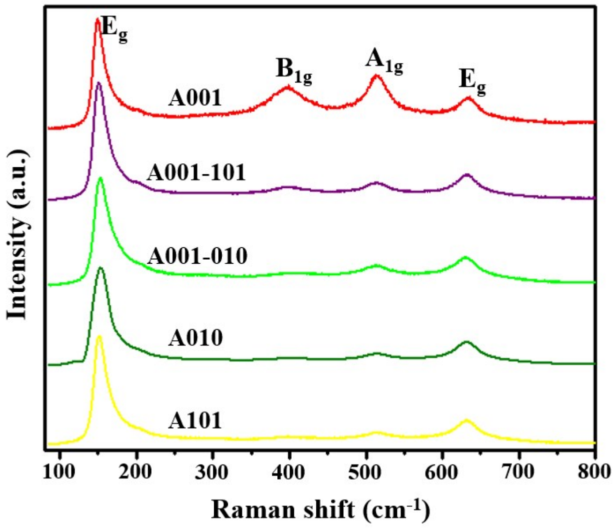

Figure S3.2 Raman spectra of various samples tested.

Similarly, Raman spectra of A001, A001-101, A001-010, and A010 are shown in Figure S3.2. Based on Equation S1, the percentage of {001} in A001, A001-101, A001-010, A010 and A101 is 84.33, 65.36, 53.96, 12.12, and 9.41%, respectively.

S4: The effect of H^+ and F^- on anatase TiO_2 in a particle form

We conducted a set of experiments to investigate whether H^+ and F^- have the same effects when applied for synthesizing anatase in a standalone particle form or in growing the structures directly on FTO substrate. We adopted the synthesizing technique reported by Wu et al.[2], which is facile and can efficiently control the facet of anatase particles, as a control experiment. In the original synthesis procedure, 10 mL of TTBT was mixed with a desirable amount of HF (0-1.2 mL) and hydrothermally treated at 200 °C for 24 h. In this study, we fixed HF at 0.5 mL and fixed the other parameters the same, and used this condition as a control experiment. Then, an extra amount of chemicals; namely, sodium fluoride (NaF), and hydrochloric acid (HCl) was separately added to the control experiment, in order to separately study the effect of F^- and H^+, respectively. The synthetic conditions are summarized in Table S4.

Table S4 The experimental conditions for studying the effect of H^+ and F^- on anatase TiO_2 in a particle form

Exp.	**37% HCl** (mL)	**NaF** (g)	**TTBT** (mL)	**HF** (mL)	**Time** (h)	**Temp.** (°C)	**Factor to study**
S4.1	0	0	10	0.5	24	200	Control Experiment
S4.2	0	**0.1**	10	0.5	24	200	The effect of F^-
S4.3	**0.5**	0	10	0.5	24	200	The effect of H^+

The resultant particles derived from the condition Exp. S4.1-S4.3 were observed by TEM, which were taken at an identical magnification (200xk), as shown in Figure S4.1-4.3, respectively.

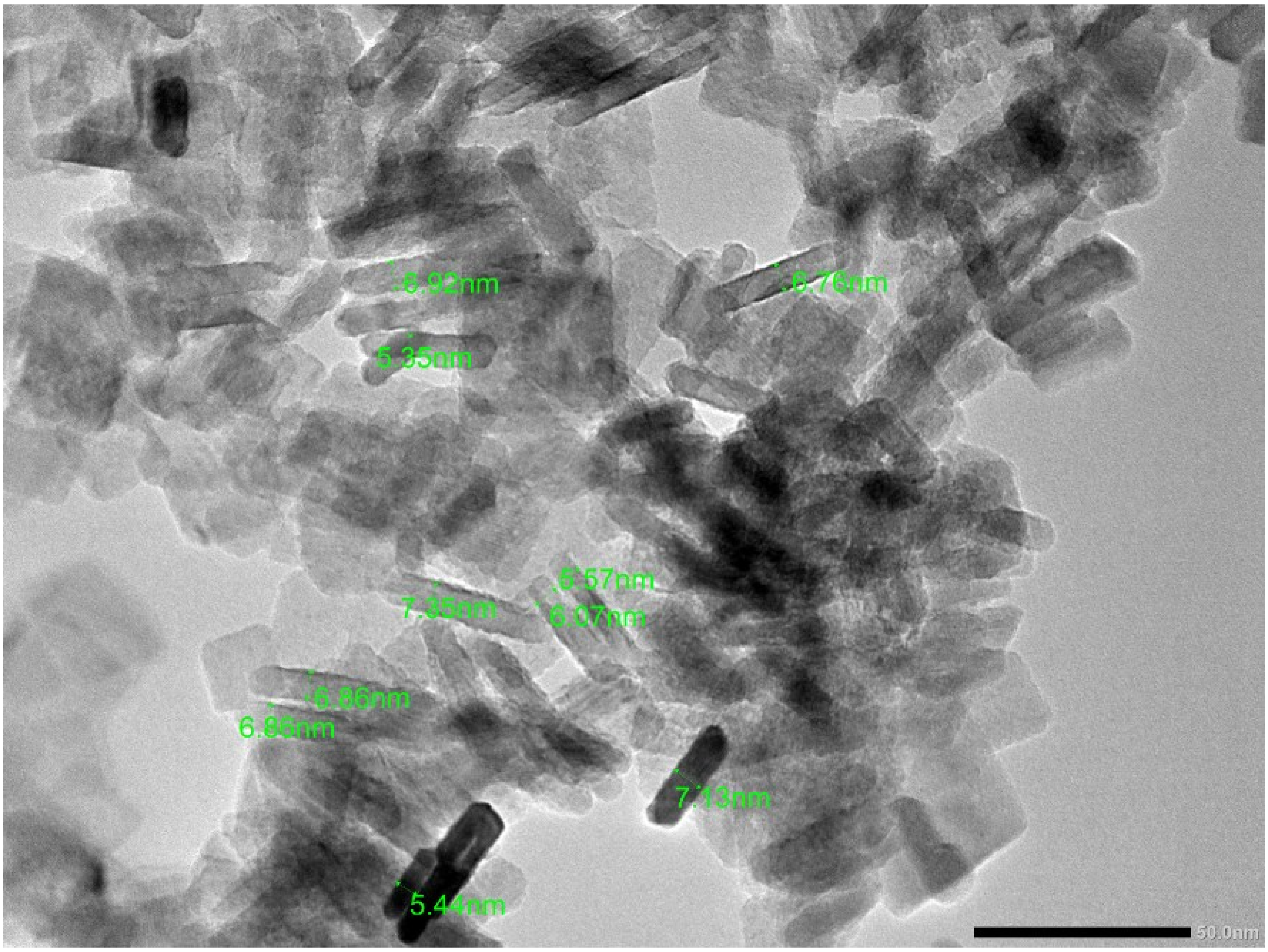

Figure S4.1 TEM image of the particles derived from Exp.S4.1 (Control Experiment)

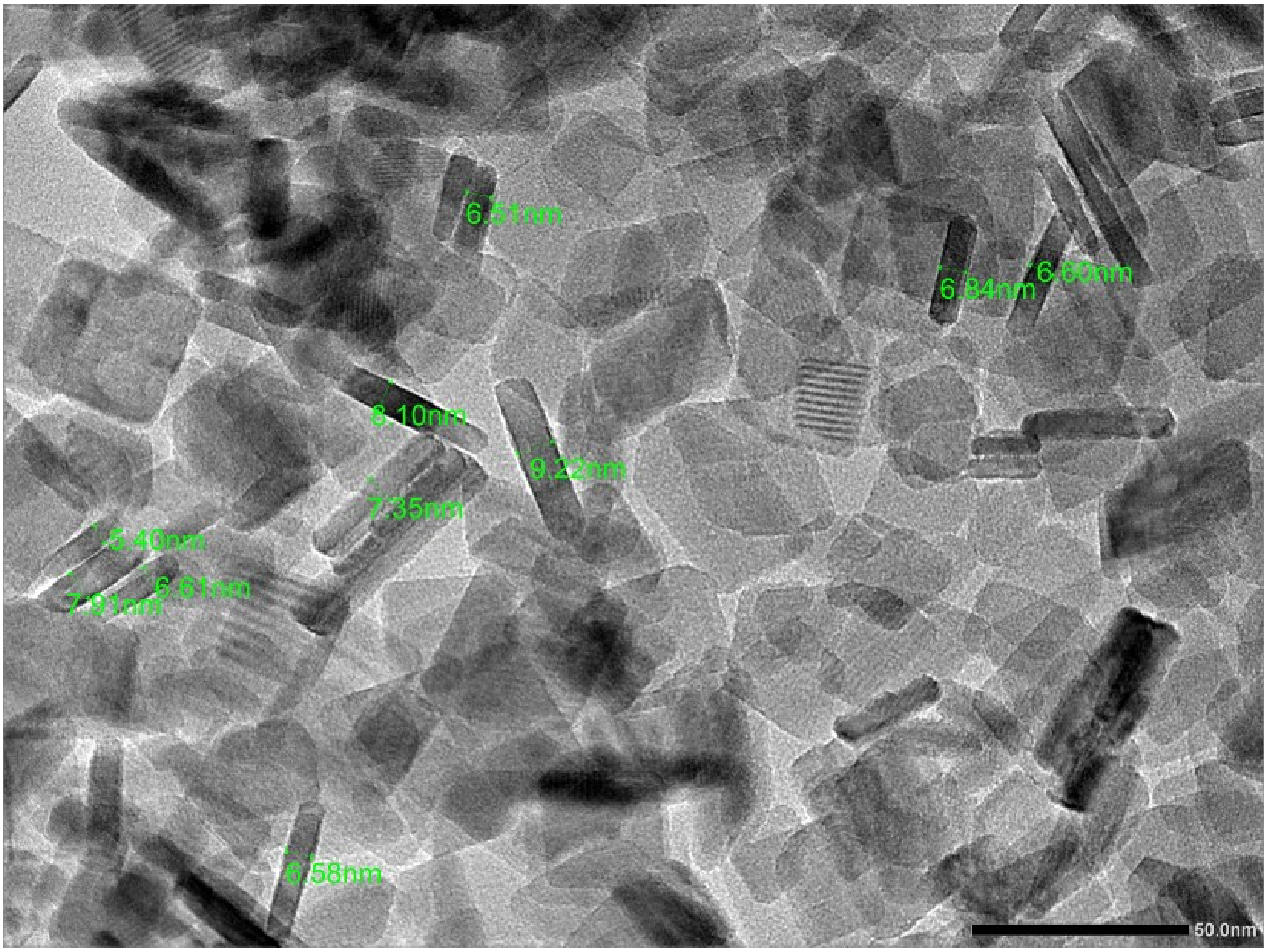

Figure S4.2 TEM image of the particles derived from Exp.S4.2 (The effect of F^-)

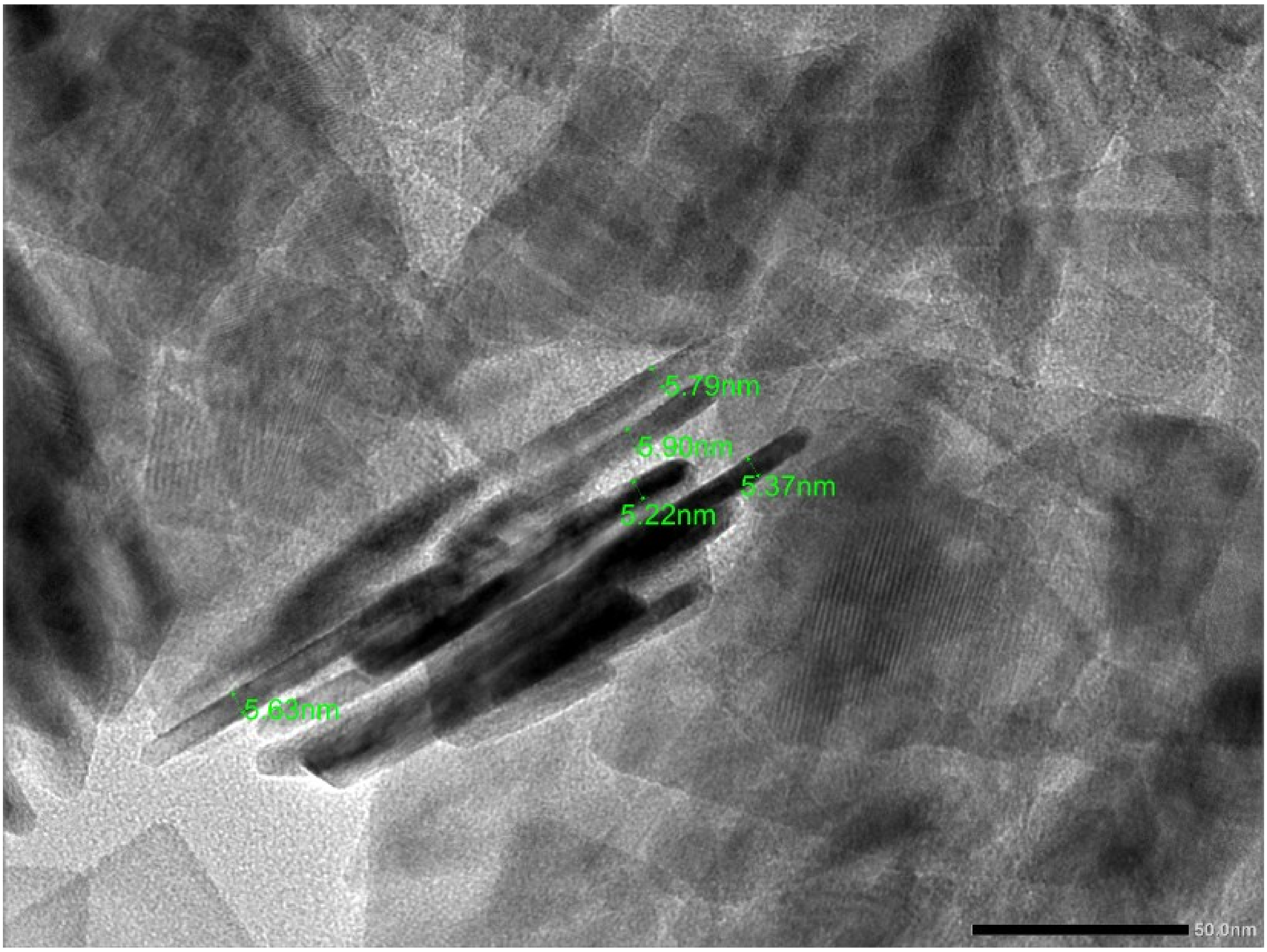

Figure S4.3 TEM image of the particles derived from Exp.S4.3 (The effect of H^+)

It was found that the average thickness of the particles derived from Exp.S4.1-S4.3 was *ca.* 6.4, 7.2, and 5.6 nm, respectively. Similar to the particles directly grown on FTO, the result suggests that H^+ and F^- play the comparable roles in controlling the morphology of anatase in a particle form in the way that H^+ ions make the particles thinner rather than F^- ions.

Moreover, lower-magnification TEM images of these samples (Figure S4.4, taken at an identical magnification, x100k) show that the width and length of the particles derived from Exp.S4.3 are much larger than that of Exp.S4.1 and Exp.S4.2. Considering that the thickness of these samples is similar (5.5-7.5 nm) but the width and length of the particles derived from Exp.S4.3 are more than three folds larger than the other two, {001} surface of the particles derived from Exp.S4.3 is thus drastically increased compared to the other two (as demonstrated in the schematic figures inset). This evidence clearly indicates that H^+ ions play a more important role in promoting the increase of {001} than F^- ions.

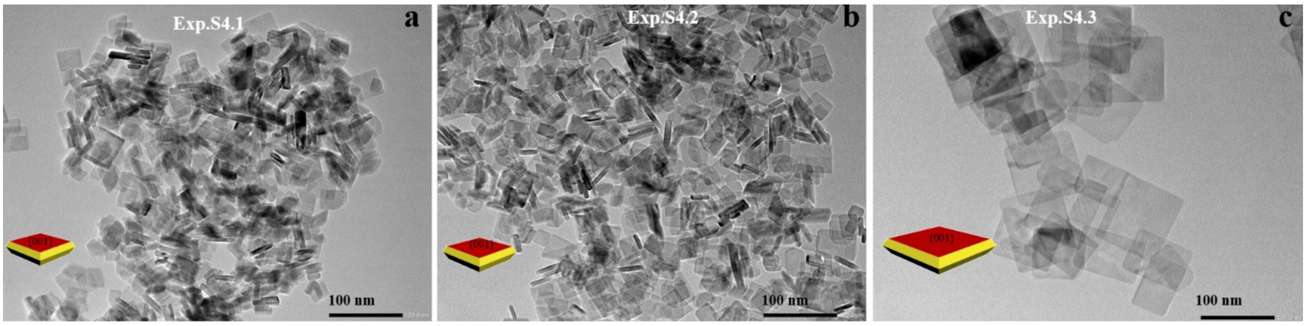

Figure S4.4 Lower-magnification TEM images taken at an identical magnification (x100k) of the particles derived from the condition Exp.S4.1 **(a)**, Exp.S4.2 **(b)**, and Exp.S4.3**(c)**, respectively.

S5: The effect of NH_4^+, and Cl^- ions in the system

S5.1: The effect of NH_4^+

To clarify whether NH_4^+ in AFT has an effect on the facet-controlled TiO_2 or not, we tried using Titanium (IV) fluoride (TiF_4) as a source of F^- ions instead of AFT. The studied conditions are listed in Table S5.1.

Table S5.1 The experimental conditions for studying the effect of NH_4^+ ions

Exp.	HCl (mL)	H_2O (mL)	TTBT (mL)	TiF_4 (g)	Time (h)	Temp. (°C)	Factor to study
S5.1.1	25	35	1	**0.2**	24	150	Effect of NH_4^+ ions
S5.1.2	25	35	1	**0.4**	24	150	
S5.1.3	25	35	1	**0.6**	24	150	

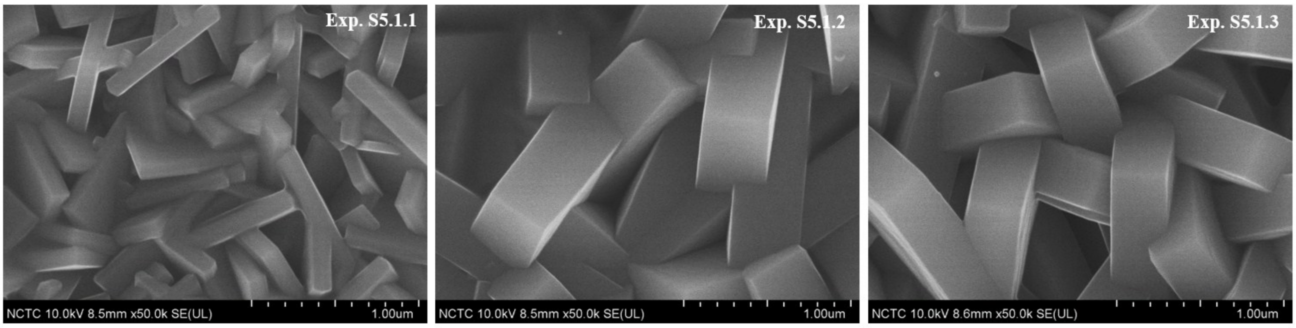

Figure S5.1 Corresponding SEM observation of the products acquired from Exp.S5.1.1-Exp.S5.1.3 in Table S5.1. All SEM images in this figure were taken at an identical magnification (50kx).

TiF_4 does not contain NH_4^+. This can ensure that the morphology of TiO_2 products is affected only by F^- ions, not NH_4^+ ions. As shown in figure S5.1, TiO_2 nanoparticles with low-index facets were also successfully synthesized. Moreover, when the amount of TiF_4 was further increased, the particle size appeared to increase. This shows a similar trend as using AFT (Exp.1-Exp.4 in S2). Clearly, these results confirm that NH_4^+ does not have a significant effect on facet-controlled TiO_2 in this study.

S5.2: The effect of Cl^-

To study whether Cl^- ions in HCl have an effect on the facet-controlled TiO_2 or not, we used the other acid (Acetic acid (glacial, Merk)) instead of HCl, and then tried adding Cl^- ions from the other source (NaCl) to the system. The designed conditions are listed in Table S5.2.

Table S5.2 the experimental conditions studying the effect of Cl^- ions

Exp.	Acetic (mL)	H_2O (mL)	TTBT (mL)	TiF_4 (g)	NaCl (g)	Time (h)	Temp. (°C)	Factor to study
S5.2.1	25	35	**1**	0.4	**0.0**	24	150	
S5.2.2	25	35	**1**	0.4	**0.2**	24	150	Effect of Cl^- ions
S5.2.3	25	35	**1**	0.4	**0.4**	24	150	

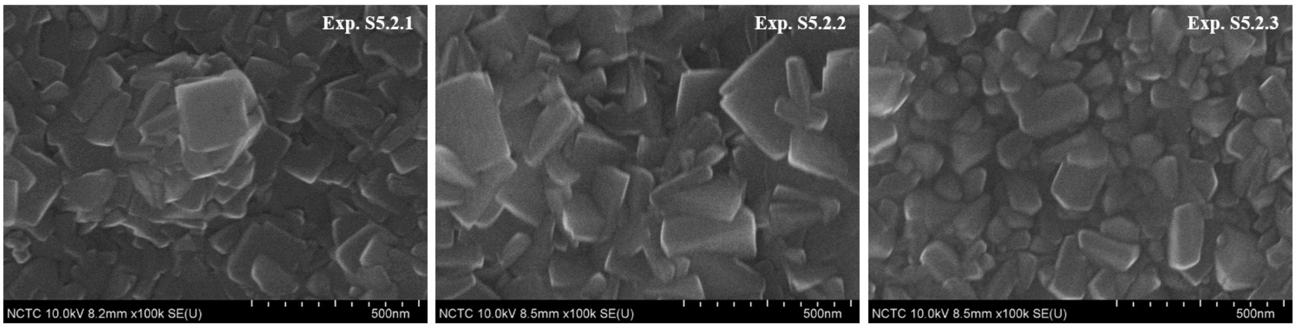

Figure S5.2 Corresponding SEM observation of the products acquired from Exp.S5.2.1-Exp.S5.2.3 in Table S5.2. All SEM images in this figure were taken at an identical magnification (100kx).

As seen from Figure Exp.S5.2.1, using acetic acid instead of HCl also successfully constructs TiO_2 crystals with facets, although the morphology of the resultants looks not well uniform. When NaCl ions were further added to the system (Exp.S5.2.3-Exp.S5.2.4), crystals exposing with facets are still observed, as shown in Figure S5.2. This evidence suggests that Cl^- in the system would not have a significant effect on controlling the facets of TiO_2 in our experiments.

However, note that not all acids can be used to synthesize TiO_2 with clear facets. For example, we also tried using nitric acid (HNO_3) and sulfuric acid (H_2SO_4), but the resultant TiO_2 particles are in irregular shapes.

S6: The effect of reaction time at low HCl (lower than 33.3 vol%)

Basically, in relatively high concentration of H$^+$, the crystal size becomes larger when the reaction time is longer. However, special attention should be taken when the concentration of H$^+$ is low, as the crystals can grow quickly and reach their full-grown in a shorter period of time. After that, where are a lot of spherical particles appearing on the surface of the crystals, as shown in Figure S6a-c. We cannot certainly conclude what crystal phase the small spherical particles is because the XRD characteristic peak of these particles is too broad, as shown in Figure S6d. However, it is expected that the small spherical particles would be $(NH_4)_3TiO_2F_5$ (PDF-1538470) and/or β-TiO_2 (PDF-0461237), as the peak is similar to the XRD peak of β-TiO_2 reported by Xiang et al. (Figure S6e) [3].

Table S6 Synthetic conditions studying the effect of the reaction time when the concentration of HCl is below 33.3 vol%

Figure	**HCl** (mL)	**H_2O** (mL)	**TTBT** (mL)	**AFT** (g)	**Time** (h)	**Temp.** (°C)	**Factor to study**
S6a	20	40	1.0	0.4	**5**	150	Reaction time (low H$^+$, AFT)
S6b	20	40	1.0	0.4	**10**	150	
S6c	20	40	1.0	0.4	**20**	150	

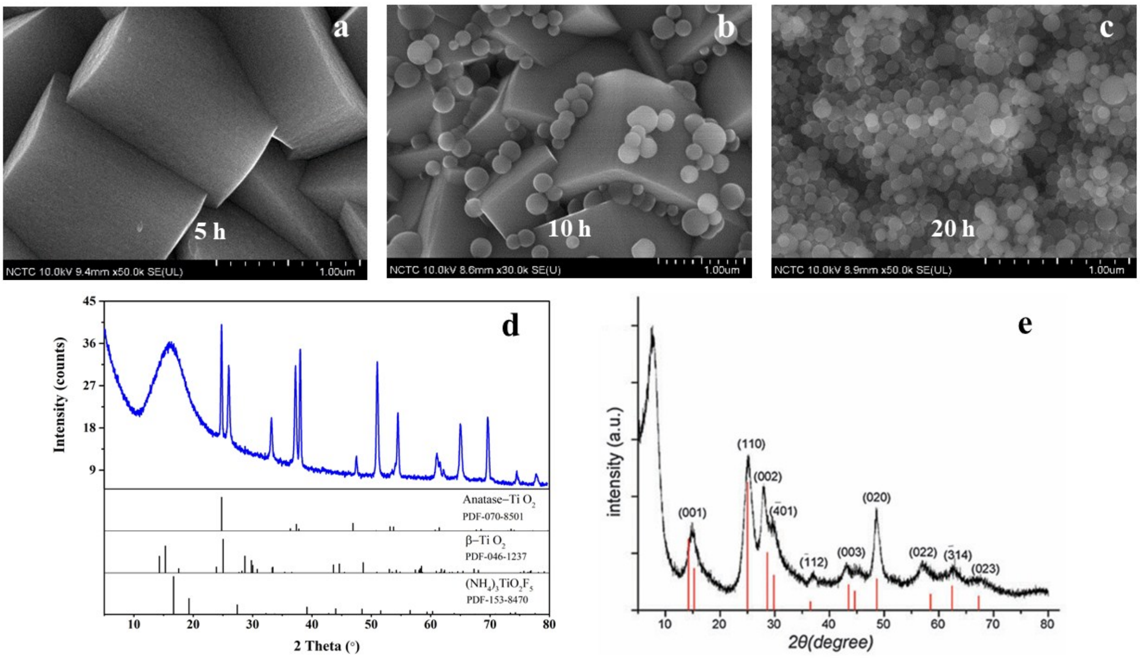

Figure S6 a-c) SEM images of the products synthesized by the condition in Table S6. All SEM images in this figure were taken at an identical magnification (30kx). **d)** XRD spectrum of the sample S6c. **e)** XRD pattern of β-TiO_2 which is derived from Reference [3] for comparison.

S7: UV-Visible light absorption and transmission spectra of various samples and their corresponding band gaps estimated by Kubelka-Munk method

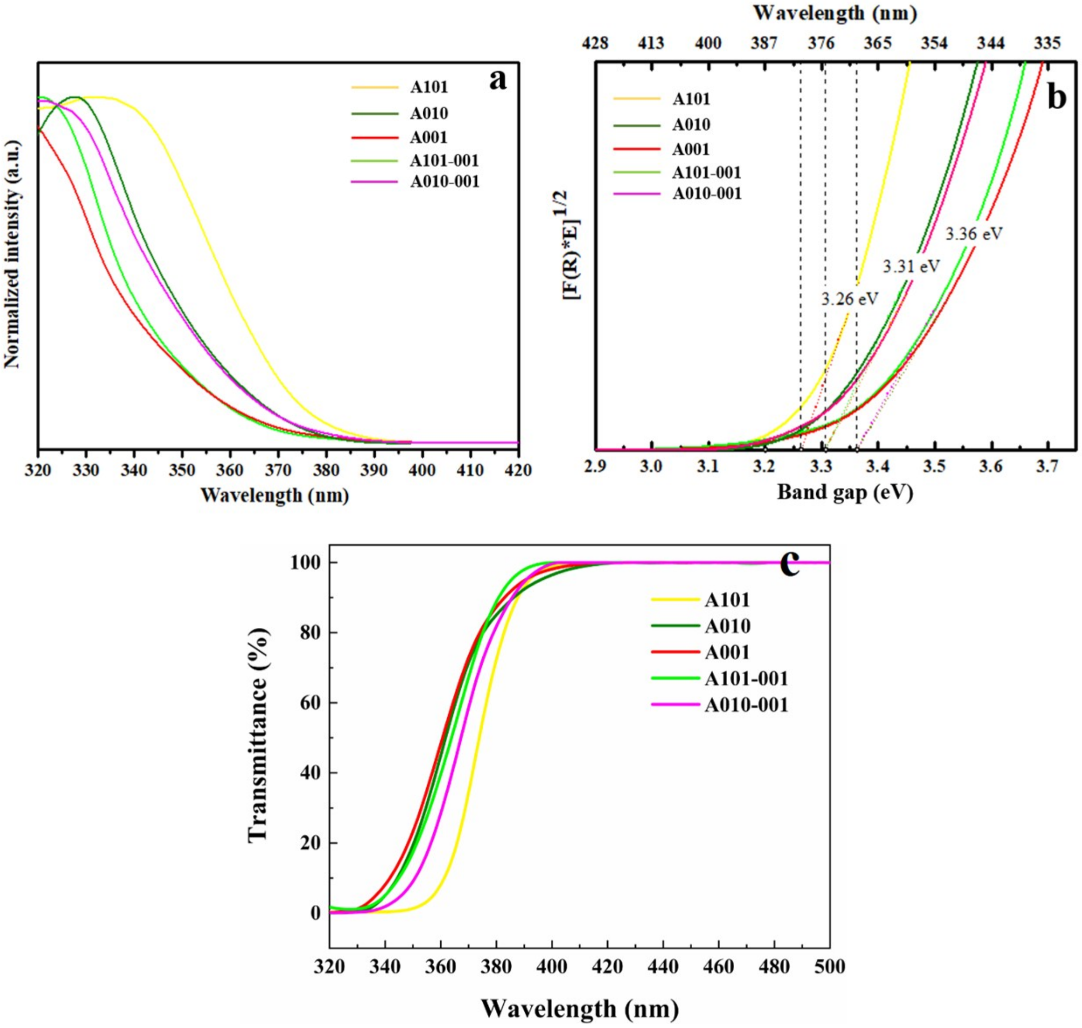

Figure S7 a) UV-Visible light absorption spectra of various samples, and **b)** their corresponding band gaps estimated by Kubelka-Munk method. **c)** transmission spectra of various samples

S8: Time-resolved gas evolution generated by various films which were tested in PEC water splitting

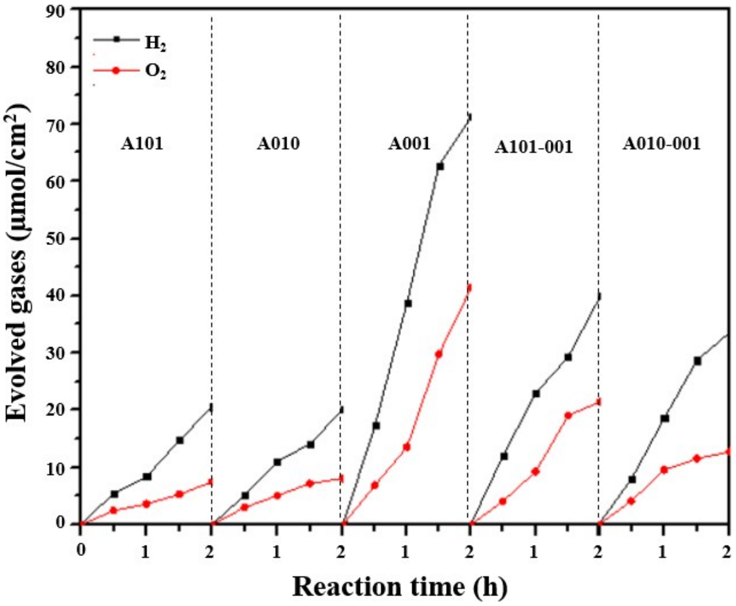

Figure S8 Evolved gases generated by various TiO_2 films dominated by different facets

S9: Summary of reduced CO_2 products generated by various TiO_2 films tested.

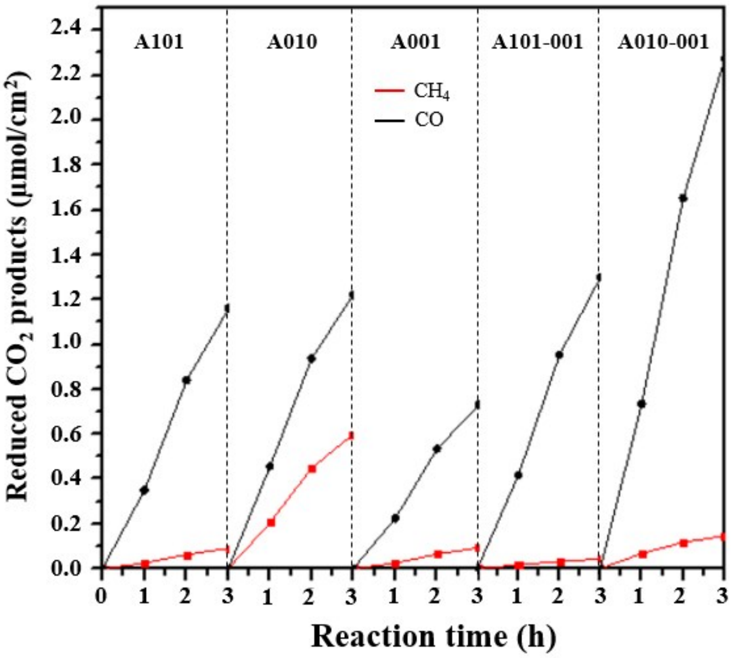

Figure S9.1 Time-resolved reduced CO_2 products generated by various films

Table S9: Summary of reduced CO_2 products generated by various TiO_2 films tested and turn over number.

Samples	**CO** (μmol.h^{-1}.cm^{-2})	**CH_4** (μmol.h^{-1}.cm^{-2})	**Total** (μmol.h^{-1}.cm^{-2})	**TON*** (h^{-1})
A101	0.387	0.030	0.417	453
A010	0.430	0.199	0.629	686
A001	0.245	0.021	0.266	184
A101-001	0.443	0.014	0.457	433
A010-001	0.758	0.049	0.807	842

*Turn over number (TON) is defined as $\frac{Number\ of\ reacted\ molecules}{Number\ of\ active\ sites}$ [4][5]. We used atomic force microscopy (AFM) to evaluate the surface area that can contact with reactants of a particular thin-film faceted electorde (Figure S9.2). Based on 10x10 μm^2 area scanned, the surface area of A101, A010, A001, A101-001, and A010-001 is 110.8, 110.4, 173.6, 127.2 and 115.4 μm^2, respectively. In other words, the surface area per 1 cm^2 of A101, A010, A001, A101-001, and A010-001 is 1.108, 1.104, 1.736, 1.272, and 1.154, respectively. The active site of TiO_2 was reported as $5x10^{14}$ cm^{-2} [6][7]. So, the number of active sites of A101, A010, A001, A101-001, and A010-001 is equal to $5.54x10^{14}$, $5.52x10^{14}$, $8.68x10^{14}$, $6.36x10^{14}$, $5.77x10^{14}$ sites, respectively. TON in this system can be calculated according to the following equation:

$$TON = \frac{[6.02x10^{23}][mole\ of\ products]}{Number\ of\ active\ sites}$$ Equation S2

As a result, TONs of various films calculated based on above mentioned data are summarized in Table S9

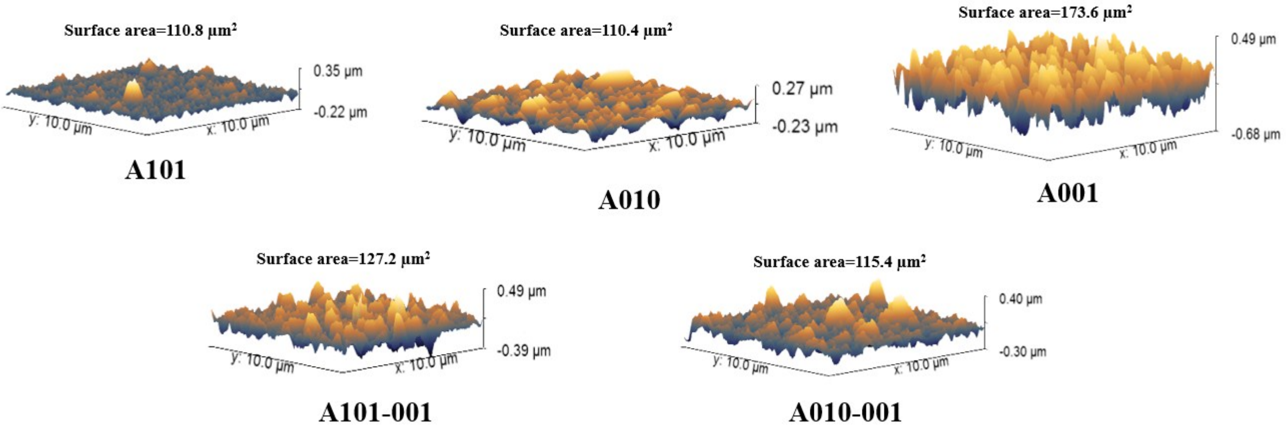

A101 **A010** **A001**

A101-001 **A010-001**

Figure S9.2 AFM images of various films for estimating the surface area of the thin-film TiO_2 photoelectrodes

S10. Model structures

The snapshots of clean structures and structures at different coverages of H^+ and F^-.

(a) rutile TiO_2(110)

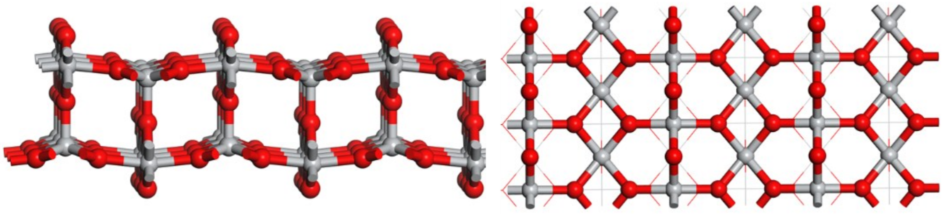

(b) anatase TiO_2(001)

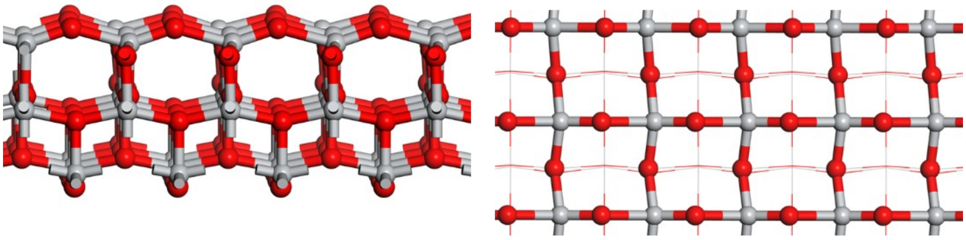

(c) anatase TiO_2(101)

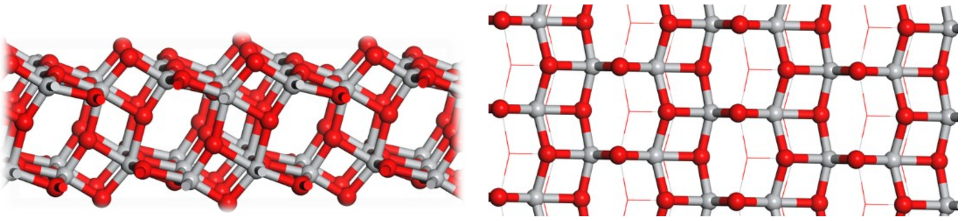

Figure S10.1 Side view and top view of the slab models (a) rutile TiO_2 (110), (b) anatase TiO_2 (001) and (c) anatase TiO_2 (101). Red and grey atoms are oxygen and titanium atoms, respectively.

rutile TiO_2 (110)

F^- coverage = 0.11 ML

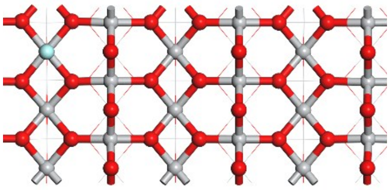

F^- coverage = 0.22 ML

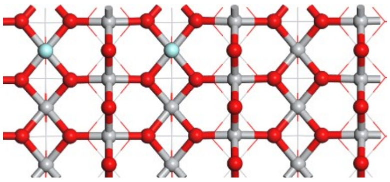

F^- coverage = 0.33 ML

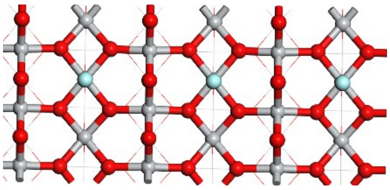

F^- coverage = 0.44 ML

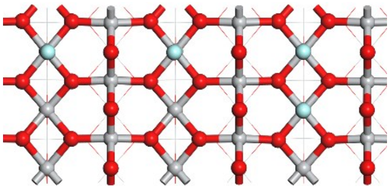

F^- coverage = 0.56 ML

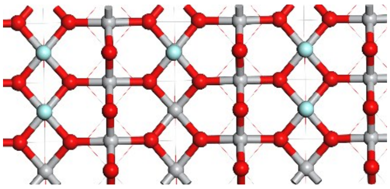

F^- coverage = 0.67 ML

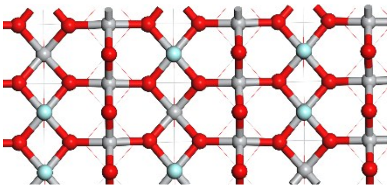

anatase TiO_2 (101)

F^- coverage = 0.13 ML

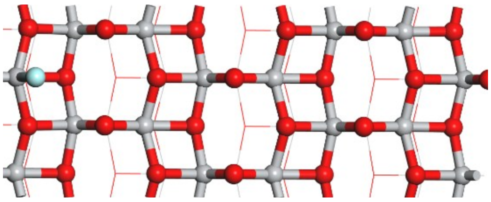

F^- coverage = 0.25 ML

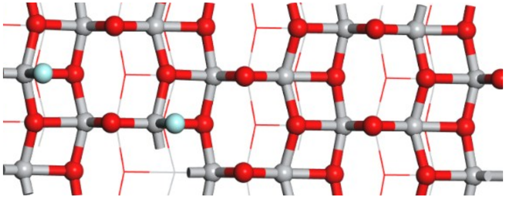

F^- coverage = 0.38 ML

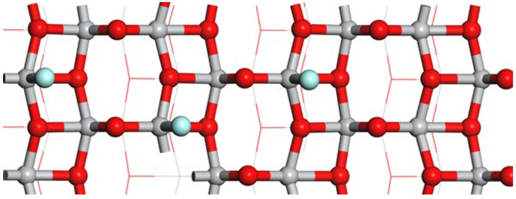

F^- coverage = 0.50 ML

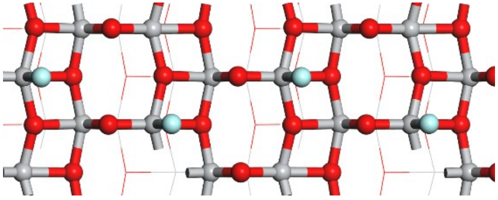

F^- coverage = 0.63 ML

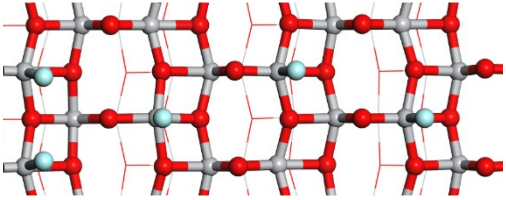

F^- coverage = 0.75 ML

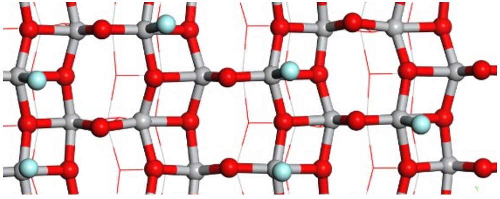

F$^-$ coverage = 0.78 ML F$^-$ coverage = 0.88 ML

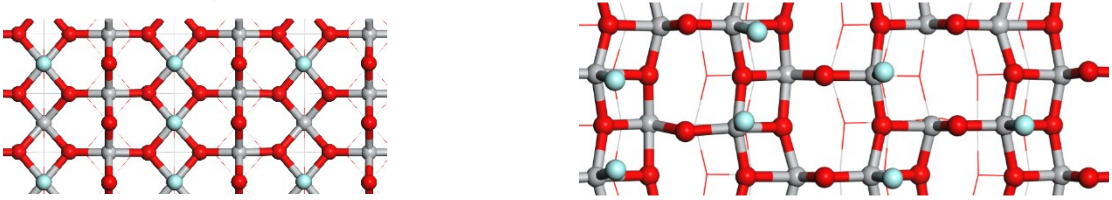

F$^-$ coverage = 1.00 ML F$^-$ coverage = 1.00 ML

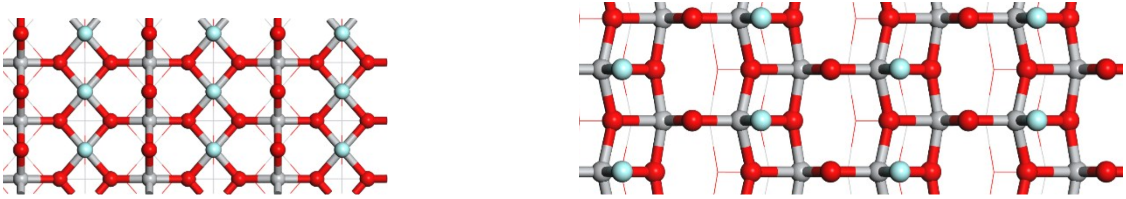

Figure S10.2. Top view of (left) rutile TiO_2 (110) and (right) anatase TiO_2 (101) with various F$^-$ coverages. Red, grey and blue atoms are O, Ti and F atoms, respectively. Surface atoms are represented by ball and stick display style and the rest are represented by line style.

anatase TiO_2 (100) anatase TiO_2 (101)

H$^+$ coverage = 0.11 ML H$^+$ coverage = 0.13 ML

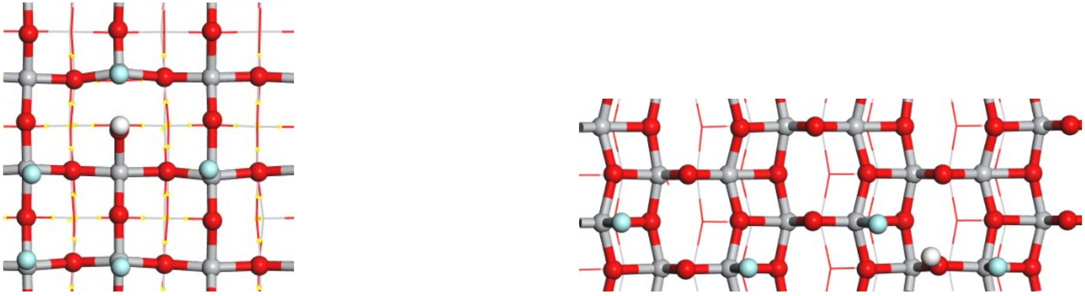

H$^+$ coverage = 0.22 ML H$^+$ coverage = 0.25 ML

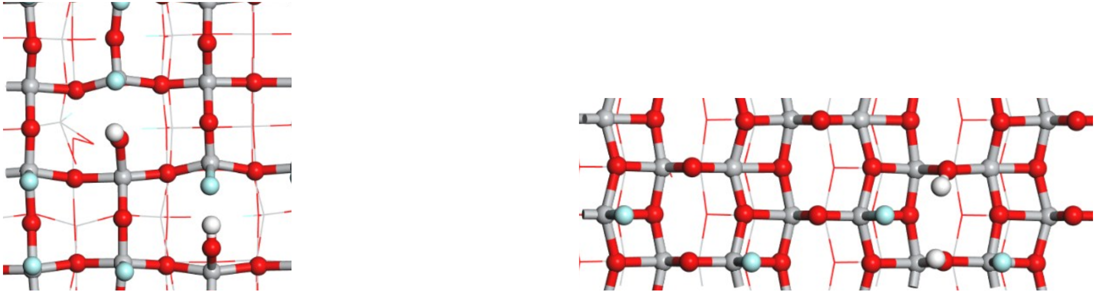

H$^+$ coverage = 0.33 ML H$^+$ coverage = 0.38 ML

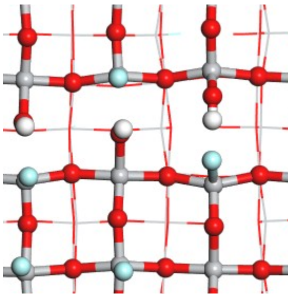

H$^+$ coverage = 0.44 ML

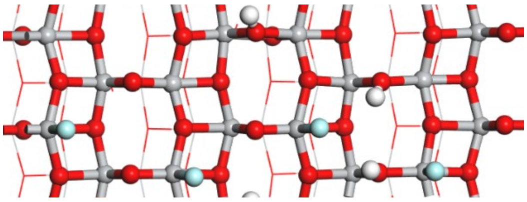

H$^+$ coverage = 0.50 ML

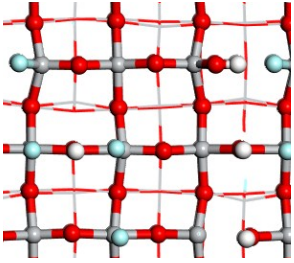

H$^+$ coverage = 0.56 ML

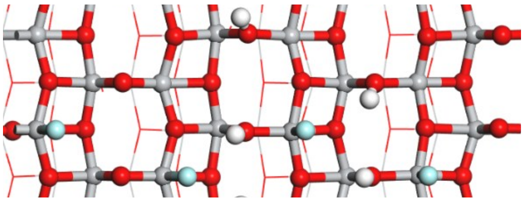

H$^+$ coverage = 0.63 ML

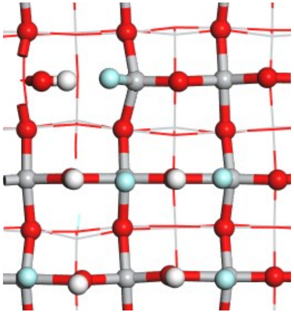

H$^+$ coverage = 0.67 ML

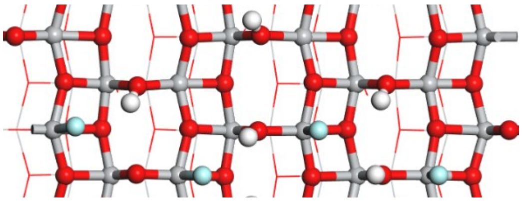

H$^+$ coverage = 0.75 ML

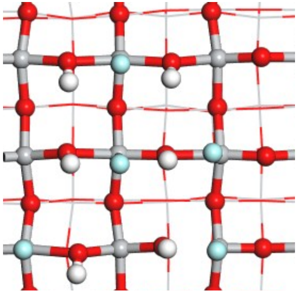

H$^+$ coverage = 0.78 ML

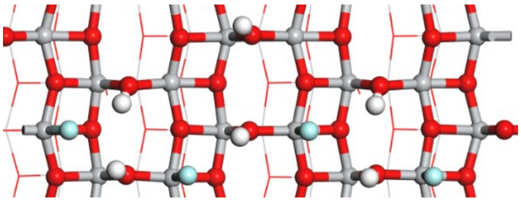

H$^+$ coverage = 0.88 ML

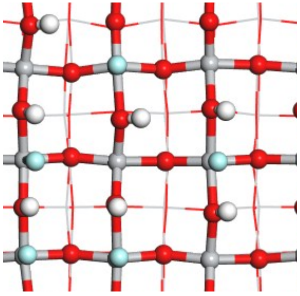

H$^+$ coverage = 1.0 ML

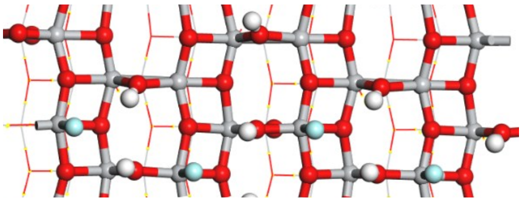

H$^+$ coverage = 1.0 ML

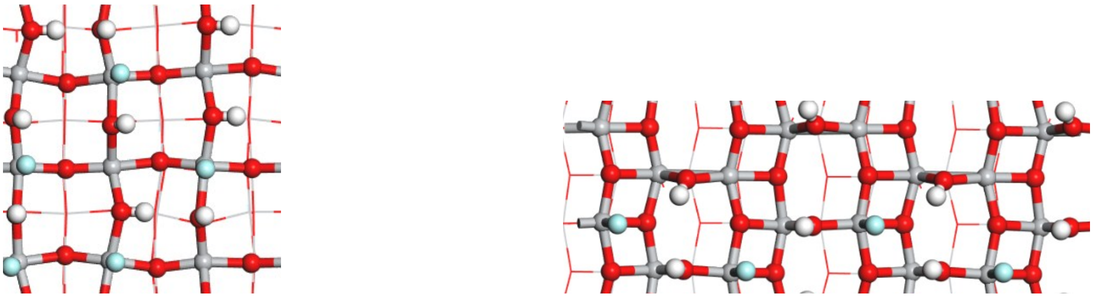

Figure S10.3. Top view of (left) anatase TiO_2 (001) and (right) anatase TiO_2 (101) with various H^+ coverages when F^- coverage is fixed at approximately 0.5 ML. Red, grey, blue and white atoms are O, Ti, F and H atoms, respectively. Surface atoms are represented by ball and stick display style and the rest are represented by line style.

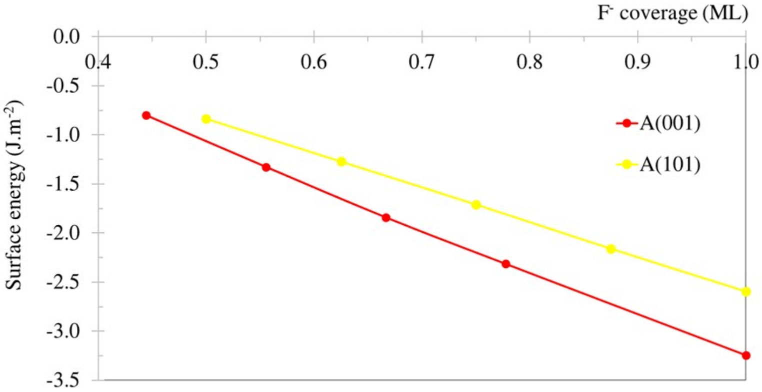

Figure S10.4. Calculated surface energies of (101) and (001) facets at various F^- coverage between 0.5-1.0 ML when H^+ coverage is fixed at 1 ML.

References (in Supplementary Materials)

[1] F. Tian, Y. Zhang, J. Zhang, and C. Pan, *J. Phys. Chem. C,* 2012, ***116***, 7515.
[2] X. Wu, Z. Chen, G. Q. M. Lu and L. Wang, *Adv. Funct. Mater.*, 2011, **21**, 4167.
[3] G. Xiang, T. Li, J. Zhoung, and X. Wang, *Chem. Commun.,* 2010, **46**, 6801.
[4] A. Kudo and Y. Miseki, *Chem. Soc. Rev.*, 2009, **38**, 253.
[5] X. Zhang, U. Veikko, J. Mao, P. Cai and T. Peng, *Chem. Euro. J.*, 2012, **18**, 12103.
[6] T. Van der Meulen, A. Mattson and L. Österlund, *J. Catal.*, 2007, **251**, 131.
[7] U. Diebold, *Surf. Sci. Rep.*, 2003, **48**, 53.